Atmos. Chem. Phys. Discuss., https://doi.org/10.5194/acp-2018-115
Manuscript under review for journal Atmos. Chem. Phys.
Discussion started: 26 February 2018

Atmospheric Chemistry and Physics Discussions

Average versus high surface ozone levels over the continental U.S.A.: Model bias, background influences, and interannual variability

Jean J. Guo[1], Arlene M. Fiore[1], Lee T. Murray[2,3,4], Daniel A. Jaffe[5], Jordan L. Schnell[6,7], Tom Moore[8], George Milly[2]

[1]Department of Earth and Environmental Sciences and Lamont-Doherty Earth Observatory of Columbia University, Palisades, NY, U.S.A.
[2]Lamont-Doherty Earth Observatory of Columbia University, Palisades, NY, U.S.A.
[3]NASA Goddard Institute for Space Studies, New York, NY USA
[4]Now at: Department of Earth and Environmental Sciences, University of Rochester, Rochester, NY, U.S.A.
[5]University of Washington, School of STEM, Bothell, WA and Department of Atmospheric Science, Seattle, WA, U.S.A.
[6]NOAA Geophysical Fluid Dynamics Laboratory, Atmospheric and Oceanic Sciences, Princeton University, Princeton, NJ, U.S.A.
[7]Now at: Department of Earth and Planetary Sciences, Northwestern University, Chicago, IL, U.S.A.
[8]WESTAR and WRAP, Colorado State University, Fort Collins, CO, U.S.A.

Correspondence to: Jean J. Guo (jean.j.guo@columbia.edu)

Abstract. U.S. background ozone (O_3) includes O_3 produced from anthropogenic O_3 precursors emitted outside of the U.S.A., from global methane, and from any natural sources. Using a suite of sensitivity simulations in the GEOS-Chem global chemistry-transport model, we estimate the influence from individual background versus U.S. anthropogenic sources on total surface O_3 over ten continental U.S. regions from 2004-2012. Evaluation with observations reveals model biases of +0-19 ppb in seasonal mean maximum daily 8-hour average (MDA8) O_3, highest in summer over the eastern U.S.A. Simulated high-O_3 events cluster too late in the season. We link these model biases to regional O_3 production (e.g., U.S. anthropogenic, biogenic volatile organic compounds (BVOC), and soil NO_x, emissions), or coincident missing sinks. On the ten highest observed O_3 days during summer (O_3_top10obs_JJA), U.S. anthropogenic emissions enhance O_3 by 5-11 ppb and by less than 2 ppb in the eastern versus western U.S.A. The O_3 enhancement from BVOC emissions during summer is 1-7 ppb higher on O_3_top10obs_JJA days than on average days, while intercontinental pollution is up to 2 ppb higher on average vs on O_3_top10obs_JJA days. In the model, regional sources of O_3 precursor emissions drive interannual variability in the highest observed O_3 levels. During the summers of 2004-2012, monthly regional mean U.S. background O_3 MDA8 levels vary by 10-20 ppb. Simulated summertime total surface O_3 levels on O_3_top10obs_JJA days decline by 3 ppb (averaged over all regions) from 2004-2006 to 2010-2012 in both the observations and the model, reflecting rising U.S. background (+2 ppb) and declining U.S. anthropogenic O_3 emissions (-6 ppb). The model attributes interannual variability in U.S. background O_3 on

O_3_top10obs days to natural sources, not international pollution transport. We find that a three-year averaging period is not long enough to eliminate interannual variability in background O_3.

1 Introduction

In the United States, ozone (O_3) is regulated as a criteria pollutant under the National Ambient Air Quality Standard (NAAQS). The current NAAQS for ground-level O_3, set in October 2015, states that the 4th-highest daily maximum 8-hour average (MDA8) O_3, averaged across three consecutive years, cannot be 71 ppb or higher (U.S. Environmental Protection Agency, 2015). The three-year average is nominally intended to smooth out fluctuations in O_3 levels resulting from natural variability in meteorology, within the timing constraints of the federal Clean Air Act for air quality planning. As even one ppb of excess O_3 may be enough to push a county out of NAAQS attainment, it is relevant to understand which sources influence the severity and timing of the highest O_3 events. As measured O_3 does not retain a signature of the source from which it was produced, estimates of background O_3 rely on models, ideally evaluated closely with observational values, to build confidence in the model capability for source attribution. Here we apply a global chemistry-transport model alongside O_3 observations to examine the highest 10 observed O_3 events, as well as average conditions, to determine which sources are influencing average versus high-O_3 events, and the extent to which they vary from year-to-year.

As U.S. anthropogenic emissions of O_3 precursors decline, the relative importance of "U.S. background" to total surface O_3 rises. U.S. background O_3 is defined here as the O_3 levels that would exist in the absence of U.S. anthropogenic emissions of O_3 nitrogen oxide (NO_x) and non-methane volatile organic compound (NMVOC) precursors. U.S. background O_3 thus includes naturally occurring O_3 as well as O_3 produced from global methane (including U.S. anthropogenic emissions) and from O_3 precursor emissions outside of the U.S.A. Jaffe et al. (2018) review the current understanding on U.S. background O_3 from models and observations, and its relevance to air quality standard setting and implementation. Previous studies estimating background O_3 over the United States found that background sources of O_3, including stratospheric O_3 intrusions (Lin et al., 2012, 2015a), increasing Asian anthropogenic emissions (Lin et al., 2015b), and more frequent wildfires in summer (Abatzoglou and Williams, 2016; Jaffe, 2011; Yang et al., 2015), may present challenges to obtaining the O_3 standard, especially since regional emission controls may be offset by a warming climate (Fiore et al., 2015). At high-altitude Western U.S. (WUS) sites in spring, the influence from stratospheric intrusions and foreign transport, combined with relatively deep planetary boundary

layers, can lead to high background O_3 events (Fiore et al., 2002; Zhang et al., 2011). Lin et al. (2017) investigated surface O_3 trends over the U.S.A. from 1980-2014 with the GFDL AM3 model and found that emissions controls decreased the 95th percentile summer O_3 values in the Eastern U.S. (EUS) by 0.2-0.4 ppb yr^{-1} over 1988-2014, but rising Asian emissions offset the effect of U.S. emissions reductions, leading to 2-8 ppb increases in monthly mean O_3 at individual sites in the WUS (Lin et al., 2016).

Earlier work in the GEOS-Chem model analyzing background O_3 during a single meteorological year noted a tendency for the model to underestimate springtime O_3 at high-altitude WUS sites but overestimate summertime O_3 over the EUS (e.g. Fiore et al., 2002, 2003; Wang et al., 2009; Zhang et al., 2011, 2014). Identifying the extent to which these biases reflect poor representation of U.S. anthropogenic versus background sources is relevant for assessing uncertainties in estimates of background O_3 on days when the O_3 NAAQS is exceeded. We build upon these prior studies by analyzing MDA8 O_3 measurements and 9-year model simulations spanning 2004-2012 from the GEOS-Chem 3D global chemistry-transport model (CTM). We use a suite of GEOS-Chem sensitivity simulations to estimate the influence from various individual background sources on O_3 concentrations and the interannual variability in background O_3 levels, with a focus on the highest 10 events in each EPA region during each summer (JJA) or year. We aim to answer the following questions: (1) Which sources exert the strongest influence on O_3 on the ten days with the highest model biases against observations? (2) Which background sources influence total O_3 the most on average versus the 10 highest O_3 days? (3) Which sources influence the interannual variability of O_3 in each region on average versus the 10 highest O_3 days?

2 Observations and model simulations

2.1 Observations

We use observed 2004-2012 MDA8 O_3 data from the EPA Air Quality System (AQS) network of urban, suburban, and rural monitoring sites, the Clean Air Status and Trends Network (CASTNet), and the Mount Bachelor Observatory (https://digital.lib.washington.edu/researchworks/browse?type=subject&value=Mt.+Bachelor+Observatory) in Oregon. MDA8 O_3 values for the AQS sites were download from http://aqsdr1.epa.gov/aqsweb/aqstmp/airdata/download_files.html#Daily (2004-2012 data last updated June 28, 2013). This dataset includes 1644 total sites from the contiguous U.S.A. from 2004-2012 with 1207 to 1333 sites

collecting data each year (U.S. Environmental Protection Agency, 2014) (Supplemental Figure 1). The number of AQS sites measuring data per year is listed in Supplemental Figure 1.

The CASTNet (ftp://ftp.epa.gov/castnet/data) O_3 monitoring sites are located in rural areas away from emission sources and densely populated regions. CASTNet sites are designed to capture background O_3 levels and characterize the broad spatial and temporal trends of air pollutants. We calculate the MDA8 O_3 concentration from hourly values at 108 CASTNet sites with data between 2004-2012, requiring at least 18 hours of data per day for each MDA8 O_3 calculation.

The Mount Bachelor Observatory, established in 2004 by the University of Washington Jaffe Research Group, is located 2.7 km above sea level on the summit of Mount Bachelor, an extinct volcano in the Cascade Mountains of central Oregon. It provides an estimate of baseline O_3 levels over the West Coast of the United States. Baseline O_3 is tropospheric O_3 concentrations at sites that have a negligible influence from local emissions (National Research Council, 2010). Here we take all hourly O_3 concentrations from Mount Bachelor and calculate the MDA8 O_3 concentrations for 2004-2012. Daily averages are included only if at least 18 hours of data are available per day. As we did not archive three-dimensional high frequency data, all MDA8 O_3 values from the model are sampled at the lowest surface layer for comparison to observation sites. Monthly MDA8 O_3 averages from Mount Bachelor are included only if at least 20 days out of the month contain valid daily data. For our comparison to monthly mean measurements at Mount Bachelor, we sample the model at the height closest to 2.7 km.

In order to evaluate the GEOS-Chem model O_3 simulation (described below in Sect. 2.3) at a spatial scale comparable to the coarse horizontal resolution global grid (2º x 2.5º), we use an available 1° x 1° grid of interpolated surface MDA8 O_3 measurements described by Schnell et al. (2014). We degrade the Schnell et al. (2014) dataset to 2° x 2.5° to match that of the GEOS-Chem simulations.

2.2 Analysis regions

Each observational site in the EPA AQS and CASTNet datasets is linked to one of the 10 EPA air quality regions (Figure 1) based on which state the site is in. The Mount Bachelor data were included with the Region 10 (Pacific Northwest) sites (Table 2) as a station representative of variations in baseline O_3 concentrations in the U.S.A. (Baylon et al., 2016) even though it is not a regulatory monitor. Similar to Reidmiller et al. (2009), we select two regions, the Southeast (Region 4) and Mountains and Plains (Region 8), as representative regions for the EUS

and WUS for illustration purposes in the main text. Figures showing our results for the other six regions are included in the supplement.

We first match each observational site to the model grid within which it falls. We then average across all sites in each region to obtain a regional MDA8 O_3 value for each day. From the regionally averaged observed MDA8 O_3, we find: (1) the ten days with the highest observed O_3 during each year (hereafter, O_3_top10obs days; similar to the definition for extreme events used in Schnell et al., 2014), (2) the ten days with the highest O_3 observations during each season (hereafter, O_3_top10obs_MAM, O_3_top10obs_JJA, and O_3_top10obs_SON), and (3) the 4th highest MDA8 O_3 within each year. In addition, we sample the model to find the ten days each year with the highest positive biases. We use O_3_top10obs as our primary metric instead of the policy-relevant 4th highest O_3 because the model bias is comparatively lower; on the days with the 4th highest values, the model bias is generally more strongly negative in the west and South Central regions and more strongly positive in the Midwest than on O_3_top10obs days (Supplemental Figure 1, Supplemental Figure 2). In addition, while the model rarely captures the exact day of the 4th highest MDA8 O_3 event, there is a 3-4 day overlap on average between the O_3_top10obs days and the highest 10 MDA8 O_3 days in the model. This overlap is similar to the 3 and 6 day overlap Jaffe et al. (2017) found in their regional models for May 1st to September 29th, 2011.

2.3 GEOS-Chem model simulations

We use the GEOS-Chem v9_02 global 3D chemical transport model (CTM) (http://www.geos-chem.org) simulations driven by Modern-Era Retrospective analysis for Research and Applications (MERRA) reanalysis meteorology from the NASA Global Modeling and Assimilation Office for 2004-2012 (Rienecker et al., 2011). The MERRA reanalysis is available at 1/2º by 2/3º horizontal resolution, which we degrade here to 2º by 2.5˚ horizontal resolution. Anthropogenic base emissions are from the Emission Database for Global Atmospheric Research (EDGAR) version 3.2-FT2000 inventory (Olivier et al., 2005) for inorganic compounds and the REanalysis of the TROpospheric chemical composition (RETRO) inventory (Hu et al., 2015; Schultz, 2007) for organic compounds. Inorganic emissions are overwritten by regional inventories for the U.S. (EPA National Emissions Inventory 2005), Canada (Criteria Air Contaminants), Mexico (Big Bend Regional Aerosol and Visibility Observational study; Kuhns and Green, 2003), Europe (European Monitoring and Evaluation Programme; Auvray and Bey, 2005), and South and East Asia (Streets et al., 2006). Separate global inventories are

used for ammonia (Bouwman et al., 1997), black carbon (Bond et al., 2007; Leibensperger et al., 2012), and ethane (Xiao et al., 2008). Anthropogenic surface emissions have diurnal and monthly variability, some with additional weekly cycles, and are scaled each year on the basis of economic data (Van Donkelaar et al., 2008). Aircraft emissions are from the Avian Emissions Inventory Code (AEIC) inventory (Stettler et al., 2011) and shipping emissions are from International Comprehensive Ocean-Atmosphere Data Set (ICOADS; Lee et al., 2011; Wang et al., 2008). Biomass burning emissions follow the interannually-varying monthly Global Fire Emissions Database version 3 (GFED3) inventory driven by satellite observations of fire activity (Giglio et al., 2010; Van Der Werf et al., 2010). Biofuel emissions are constant (Yevich and Logan, 2003). Biogenic VOC emissions from terrestrial plants follow the Model of Emissions of Gases and Aerosols from Nature (MEGAN) scheme version 2.1 (Guenther et al., 2012) and vary with meteorology (Barkley et al., 2011). Emissions of NO_x from soil microbial activity follow Hudman et al. (2012). Methane surface concentrations are prescribed each month using spatially interpolated surface distributions from NOAA Global Monitoring Division flash data.

We first perform a base simulation (O_3_Base) in which all emissions are prescribed normally for 2003-2012. We then perform parallel sensitivity simulations in which we remove individual sources (Table 1), including (1) U.S. anthropogenic emissions, but maintaining present-day methane concentrations; the O_3 in this simulation provides an estimate of U.S. background O_3 (hereafter, O_3_USB); (2) an otherwise identical simulation that also excludes those emissions from Mexico and Canada, O_3 in this simulation is referred to as "North American Background" O_3 (O_3_NAB); (3) wildfire emissions, (4) biogenic VOC emissions, (5) Soil NO_x, and (6) Lightning NO_x. In addition, we perform a "natural" simulation in which all anthropogenic emissions have been removed globally and methane is prescribed at preindustrial levels to provide an estimate of "natural" O_3 (O_3_NAT). In all simulations, we discard 2003 from our analysis as initialization. We estimate the contribution of each individual sector to the total concentration by subtracting the O_3 in each sensitivity simulation in which that source has been removed from the O_3_Base simulation. As in all "zero-out" perturbation simulations, non-linearities in atmospheric photochemistry make this a simple estimate of the contribution of each source, and the contribution of each source depends on the presence of all other precursor emissions at present-day levels (e.g., the impact of BVOCs emissions is sensitive to the amount of anthropogenic NO_x emissions). Hereafter, the terms listed in the "Notation" column of Table 1 will be used to refer to the influence of each source on total O_3 (O_3_Base). Note that this set of model simulations does not directly isolate stratospheric O_3 or Asian influences. Previous work has shown that

stratospheric O_3 can increase O_3 levels by 17-40 ppb in the WUS in spring when MDA8 O_3 levels are 70-85 ppb, and Asian emissions can contribute 8-15 ppb to MDA8 O_3 on days above 60 ppb (Lin et al., 2012, 2015a). Stratospheric and Asian influences are included as part of our O_3_USB estimates; Asian influences are included in O_3_ICT+CH_4, and O_3_NAT contains the influence of stratospheric O_3 along with natural biogenic precursor emissions, wildfires, and lightning NO_x.

3 Model evaluation

3.1 MDA8 O_3 distributions

Previous studies have found that averaging all observational sites within a model grid cell tend to disproportionately represent urban stations, especially when looking at high O_3 days (Schnell et al., 2014). To evaluate the ability of our coarse resolution model to capture observed high-O_3 events, we compare the MDA8 O_3 simulated by GEOS-Chem to the observations in two ways. First, we use the Schnell et al. (2014) gridded dataset degraded to the model resolution. Second, we compare each individual observational site to the model grid cell within which it resides. The model is biased positively with either method (Figure 2a, b), but the shape of the model distribution constructed with the latter approach (Figure 2b) better matches the observed distribution than that of the former (Figure 2a). Matching individual sites to the nearest model grid (Figure 2b) results in a better estimate of high-O_3 days; the model overestimates the percentage of days above 70 ppb by about three times when we match to individual measurement sites (3.14% of days are above 70 ppb in the observations versus 9.92% in model) but by about ten times in comparison to the re-gridded Schnell (2014) dataset (0.37% of days are above 70 ppb in the observations versus 3.91% in the re-gridded dataset).

3.2 Baseline O_3 at Mount Bachelor

Mount Bachelor Observatory is located at 2.7 km above sea level, where it regularly samples free tropospheric O_3 and is rarely influenced by local anthropogenic emissions (Reidmiller et al., 2009). It is therefore, a valuable site for examining baseline O_3 values. Figure 3 compares modeled and observed monthly mean O_3 at Mount Bachelor. The observations peak in springtime and then fall in the summer months. The model, however, has a maximum in and underestimates springtime baseline O_3. We infer, consistent with our analysis below, that the model does not resolve springtime high-O_3 events, possibly reflecting an underestimate of stratospheric influences (see Fiore et al., 2014; Zhang et al., 2011; 2014). The model indicates that O_3_USB dominates O_3_Base (Figure 3).

Even at this baseline site, however, the model indicates that U.S. anthropogenic emissions enhance monthly mean O_3 by at least a few ppb (estimated as the difference between O_3_Base and O_3_USB).

3.3 Magnitude and timing of high-O_3 events

Simulated seasonal mean MDA8 averaged over the full 2004-2012 period is higher than observed by 5-30 ppb (Figure 4a, b, c), with the largest biases typically occurring in the Northeast and Midwest. The model bias is highest in summer (JJA) (15-30 ppb at most sites), followed by fall (SON) (10-20 ppb) (Figure 4a, b, c). Recent work in a newer version of GEOS-Chem attributes some of the positive model bias in the EUS to excessive NO_x emissions in the 2011 National Emission Inventory (NEI) (Travis et al., 2016), an inability of the model to resolve vertical mixing in the boundary layer, and a weak response to cloud cover (Travis et al., 2017). The model is closest to the observations in spring, with a positive bias usually <10 ppb over the eastern states and generally within ±5 ppb over most western sites (Figure 4a, b, c). On O_3_top10obs days, however, biases are typically lower than on average days (Figure 4, Table 3; see also year-by-year maps in Supplemental Figure 1). At some WUS sites, the model underestimates O_3 levels during the highest events by 10-20 ppb. We note that the model systematically underestimates O_3 in the Central Valley of California in all three seasons, which we attribute to the inability of the coarse model resolution to resolve topographical gradients and valley circulations (or stagnation) in this region which experiences some of the highest observed O_3 in the nation.

We compare the MDA8 O_3 distributions in the observations versus the model (O_3_Base) during the 10 most biased days in each of the ten regions across the nine years (900 total events). These “most-biased” days in the model tend to fall around the observed median (Figure 2c) during the warm season (June - October), with almost 40% of the days falling in August alone (Figure 5), and are 9-45 ppb higher than the observations (circles in Figure 6, Supplemental Figure 3). We analyze the perturbation simulations (Table 1) to identify which sources influence simulated O_3 most strongly on the “most-biased” days versus on average (i.e., all 365 or 366 days), which we assume are also likely the main drivers of the bias. In all regions, the largest sources on the “most-biased” model days are O_3_USA (3-30 ppb higher MDA8 O_3 than on average with the exception of the Pacific SW where O_3_USA is smaller than on average days), O_3_BVOC (by 1-15 ppb), and O_3_SNO_x (by 1-10 ppb; Figure 6, Supplemental Figure 3). By contrast, O_3_ICT+CH_4 is up to a few ppb higher on average days than on the most-biased model days. The 10 most biased days in the model tend to be 10°C warmer than average (Figure 6,

Supplemental Figure 3), contributing to the higher O_3_BVOC and O_3_SNO_x. We emphasize that O_3_USA and O_3_BVOC are not additive as anthropogenic NO_x reacts with biogenic VOC to produce O_3.

To explore possible drivers of model biases across the different seasons, we evaluate the timing of the highest ten events across each year in the O_3_Base, O_3_USB, and O_3_noBVOC (BVOCs shut off) simulations for each region (900 events). We bin these 900 events by month and calculate the percentage of the total events that fall within each month. Note that all the top ten days fall between March and October. The standard model (O_3_Base) underestimates the occurrence of high events early in the O_3 season (March-June) and overestimates them later in the season (July-September) (Figure 7). While the model indicates that most top ten O_3 days fall between July-August (35% each), the observations show that May through August each contain around 15-25% with the maximum in June at 25%. When we examine the highest ten O_3 events in the O_3_USB case (U.S. anthropogenic emissions shut off), we see 5-10% fewer top ten events in July and August (27% in July and 28% in August), suggesting that O_3_USA is contributing most to the temporal shift (and general summertime overestimate) relative to the observations. The O_3_USB case does capture some early spring events in April (5%) and May (10%), though still fewer than observed (12% and 17% respectively). In the O_3_noBVOC case, there are 5-10% more events during April and May than in the O_3_Base case, but the shortage of high spring O_3 events remains. The lack of high events in spring may stem from the springtime underestimate in this model, particularly at high altitude sites (e.g., Figure 5; see also Figures 4 and 6 of Fiore et al. (2014)), and may reflect poor representation of stratospheric O_3 intrusions at the coarse resolution of the CTM (Zhang et al., 2014). The summertime overestimate of high-O_3 events is less pronounced in the O_3_noBVOC case than in the O_3_Base case, implying that BVOCs are also contributing to the misplaced seasonal timing of the highest events, either through excessive O_3 production or a missing coincident sink. For example, Makar et al. (2017) suggest that failing to represent canopy turbulence and shading effects on photolysis can lead to high-O_3 biases in models.

3.4 Interannual variability

Figure 8 shows the Pearson correlations coefficients (r) between monthly average observed and O_3_Base values from 2004-2012. In May, correlations are generally strong ($r \geq 0.9$) in the Mid-Atlantic and Southeast regions, but much lower ($r = 0.2$) in the New England region. This pattern may reflect shortcomings in representing the onset of BVOC emissions. In July, the regions flip, with lower correlations in the Southeast and higher

correlations in New England. At some sites in the WUS, lower correlations occur during summer months, which may be tied to excessive influence from lightning NO_x advected from Mexico (see also Zhang et al., 2011; 2014) or anomalous events such as wildfires that are not well-captured by the model.

In general, correlations only average about $r = 0.2$ in the winter and early spring over much of the United States (Supplemental Figure 4); the drivers for these weak correlations may be connected to the model tendency to underestimate the occurrence of springtime high-O_3 events. From May to September, however, the months during which high-O_3 events are most likely to occur, the correlation between 2004-2012 observed and simulated O_3 monthly averages over much of the contiguous United States exceed $r = 0.7$ (Figure 8, Supplemental Figure 4). We conclude that the model broadly captures monthly variations from year-to-year during the warm season and can thus be applied to interpret the role of background sources in contributing to interannual variations during most of the high-O_3 season. We note that Clifton et al. (2017) found that the GEOS-Chem model does not capture interannual variability in deposition velocities observed at Harvard Forest, MA, but it is unclear to what extent this process would amplify or dampen interannual variability associated with changes in emissions.

4 Influence of individual sources on average versus high-O_3 days

In Tables 3 and 4, we report the influence of the O_3 sources defined in Table 1 on average versus O_3_top10obs days separately for spring (MAM), summer (JJA), and fall (SON) (ten days from each of the nine simulation years for 900 events for each region and season). We also report the difference in source influences between average and O_3_top10obs days, which we interpret as the enhancement from that source relative to average conditions.

We first consider the average ranges in MDA8 O_3 contributed by the various sources. Both O_3_USA and O_3_USB tend to follow the seasonal cycle of O_3_Base, with highest abundances in summer. The model indicates that O_3_USB is 30-60 ppb (range over regions) during summer and highest over the WUS. O_3_USA is generally 20-30 ppb over the EUS in summer, but only 10-20 ppb over the WUS. O_3_ICT+CH_4 averages 2-13 ppb over all regions and is highest in spring (8-13 ppb compared to 2-11 ppb in summer and 6-12 ppb in fall) (Table 4, Figure 9, Supplemental Figure 5). O_3_NALNO$_x$ has a relatively minor influence (at most 1.5 ppb) in all regions and seasons. The influence from O_3_CA+MX is generally less than a couple of ppb.

Atmos. Chem. Phys. Discuss., https://doi.org/10.5194/acp-2018-115
Manuscript under review for journal Atmos. Chem. Phys.
Discussion started: 26 February 2018

Atmospheric Chemistry and Physics Discussions

We interpret the "difference" lines in Tables 3 and 4 as the enhancements from each source on high days in each season (O_3_top10obs_MAM, O_3_top10obs_JJA, O_3_top10obs_SON) relative to average conditions. Over all regions, O_3_BVOC and O_3_SNO_x influence O_3_Base more on O_3_top10obs days (for all seasons) than on average days whereas O_3_ICT+CH_4 is typically lower by up to 3 ppb on O_3_top10obs days (for all seasons) than on average days (Table 3, Table 4, Figure 9, Supplemental Figure 5). O_3_USA is 8-11 ppb higher on O_3_top10obs_JJA days versus average days over the New England, NY+NJ, Mid-Atlantic, Midwest, and South Central regions, but only up to 5 ppb higher over other regions (Table 3, Figure 9, Supplemental Figure 5). The model indicates an even stronger anthropogenic enhancement (up to 19 ppb) on O_3_top10obs_SON days in some EUS regions (Table 3). O_3_USB is enhanced on O_3_top10obs_JJA days by 2-12 ppb relative to average days, with the smallest enhancements occurring in the Mid-Atlantic, Southeast, and Midwest regions, and the largest enhancements occurring in the Pacific NW. In contrast to all the other regions, O_3_USB is the dominant source enhancing O_3_top10days_JJA over the Mountains and Plains, Pacific NW, and Pacific SW regions (4-12 ppb for O_3_USB but < 5 ppb from either O_3_USA or O_3_BVOC). In line with earlier work reviewed by Jaffe et al. (2017), enhanced O_3_USA dominates O_3_top10obs_JJA days over much of the U.S.A., whereas in the WUS, O_3_USB enhancements exceed O_3_USA enhancements on O_3_top10days_JJA. O_3_BVOC enhances O_3_top10obs days (for all seasons) by up to 9 ppb, with the influence often largest in fall (when O_3 formation is more sensitive to VOC; e.g., Jacob et al., 1995). We re-emphasize that BVOCs contribute both to O_3_USA when reacting with anthropogenic NO_x and to O_3_USB when reacting with all other NO_x sources. In contrast to the sources discussed above, O_3_ICT+CH_4 influences average days by up to a few ppb more than on O_3_top10obs days (for all seasons), with the largest differences between average and high days occurring in EUS regions (1-3 ppb lower on O_3_top10obs days (for all seasons) in New England, NY+NJ, Mid-Atlantic; Table 4, Figure 9, Supplemental Figure 5). O_3_$NALNO_x$ is at most 2 ppb higher than average on O_3_top10obs days. The O_3_CA+MX influence is roughly equivalent (generally to within a ppb) on average versus O_3_top10obs days during all seasons (Table 4).

5 Interannual variability in the sources influencing high vs. average ground-level O_3

Despite its high mean bias and seasonal phase shift, the model does capture some of the observed interannual variability in observed O_3_top10obs_JJA MDA8 O_3 concentrations (Figure 8, Supplemental Figure 6; r = 0.5 to $\geq$ 0.9). Comparing the 2004-2006 period with 2010-2012, both observed and simulated MDA8 O_3

concentrations on O_3_top10obs_JJA days hold steady or decrease across all regions. This change reflects opposing influences in the model: rising O_3_USB (by 2 ppb averaged over all regions) and declining O_3_USA concentrations (by 6 ppb averaged over all regions) (Figure 10, Table 5, Supplemental Figure 6). We note that over the Pacific NW there is a 4 ppb decrease in O_3_USB from 2004-2006 to 2010-2012. Within the ten regions, the model captures the sign of the changes in MDA8 O_3 over this period but not the magnitude (Table 5). We emphasize that the 2010-2012 period includes two of the warmest years on record (Figure 10). Figure 10 shows that O_3_NAT tracks with O_3_USB, indicating that the year-to-year variability in O_3_USB is primarily driven in the model by meteorology as opposed to variability in upwind international anthropogenic emissions. O_3_USB and O_3_NAT on O_3_top10obs_JJA days generally track meteorological changes, with dips in MDA8 O_3 occurring during years with cooler temperatures (2008-2009) and increases in years with warmer temperatures (2011-2012) (Figure 10, Supplemental Figure 6). Note that although 2012 was the hottest year on average between 2004-2012 (except in the Pacific NW where 2004 was warmer by around a degree), it was not the hottest summer in all regions.

Year-to-year variations in monthly average O_3_USB are relatively large, with 10-15 ppb differences between the highest and lowest O_3_USB years during the warmest months (Figure 11, Supplemental Figure 8). Seasonal variations also differ by region, especially during summer. For example, the western U.S. regions have a smooth seasonal cycle with O_3_USB concentrations rising from January to a peak in July and August, and then declining again. Interannual and seasonal variability in O_3_USB are generally greater in the Southeast than in the Mountains and Plains, and Plains regions (Figure 11, Supplemental Figure 8). Year-to-year variability in O_3_BVOC is smaller than O_3_USB, with a maximum range of about 10 ppb between the highest and lowest years during August. O_3_SNOx ranges by a few ppb throughout the summer in the Southeast, and by up to 6 ppb over the Mountains and Plains in August (Figure 11).

O_3_USA anomalies relative to the 2004-2012 average illustrate declining influence in all regions, with negative anomalies after 2007 on both O_3_top10obs and average days (Figure 12, Supplemental Figure 5). This finding is well established by earlier work demonstrating decreases in high-O_3 concentrations as a result of regional NO_x emissions reductions over the past few decades (Cooper et al., 2012, 2014a; Jaffe et al., 2017; Young et al., 2017). O_3_BVOC is the main driver of the high and low O_3 anomalies (up to ±5 ppb on O_3_top10obs_JJA days) from year-to-year.

Specific events can affect O_3 in any given year. For example, in 2008, there were extensive fires across much of California in May, June, and July. In 2008, the Pacific SW region that includes California, Nevada, and Arizona, shows a positive anomaly in O_3_BB (> 1 ppb) on the O_3_top10obs days, stronger than during any other year in that region (Supplemental Figure 11). If we restrict our analysis solely to Reno, NV, the anomaly for O_3_BB was 7 ppb in July 2008 relative to the 2004-2012 July average (not shown). We emphasize that a single location can be more strongly influenced by a specific source than the regional averages on which we have focused.

Currently, the U.S. EPA uses a 3-year averaging period. We evaluate here the extent to which the 3-year averaging period removes interannual variability in meteorology (the grounds for the averaging). In Figure 13 (and in Supplemental Figure 12, Supplemental Figure 13), we examine the range for each region on the O_3_top10obs days between 2004-2012 in the observations, O_3_Base, and O_3_USB. The dots indicate where the 4th-highest MDA8 O_3 day fell for each simulation. For the 2004 to 2012 period, the range of the three-year averages of the observations is a few ppb lower than the annual range covered by the 10 highest events (Figure 13, Supplemental Figure 12, Supplemental Figure 13). The annual range in the model (O_3_Base) sampled on O_3_top10obs days tends to be wider than the observed range (except for a few years in New England and NY+NJ) by as little as a few ppb to as much as 20 ppb. This modeled range overestimate lessens when averaged over three years (Figure 13a, b versus Figure 13c, d). We also include in Figure 12 (and Supplemental Figures 12 and 13) the range of the O_3_USB on the O_3_top10obs days. While the three-year averaging period reduces the range in O_3_USB on the highest days, variability remains, and over the Mountains and Plains regions this O_3_USB is the dominant source influencing these high days (Figure 13b, d). We conclude that a three-year smoothing period is not long enough to eliminate entirely the interannual variability in background MDA8 O_3 levels.

6 Conclusions

As air quality controls decrease U.S. anthropogenic precursor emissions to O_3, the relative importance of the background influence on total surface O_3 increases. We use O_3 MDA8 concentrations spanning 2004-2012 from the EPA AQS, CASTNet, and Mount Bachelor Observatory sites, and various sensitivity simulations from the global GEOS-Chem 3D chemistry transport model to estimate the influence from various individual background sources on O_3 in each of the ten EPA regions in the continental U.S.A. We examine differences between background and U.S. anthropogenic influences on average- and high-O_3 days and on interannual variability. Correlations between monthly

averages across 2004-2012 show that the model captures monthly variations from year-to-year, especially during summer (JJA). We find that the extent to which the current three-year averaging period for assessing compliance with the National Ambient Air Quality Standard for O_3 succeeds in smoothing out interannual variability depends on the range in consecutive years, and thus varies by region and time period, but is generally not long enough to completely eliminate the interannual variability in background O_3 (Figure 13).

We find substantial biases in the severity (+0-19 ppb in maximum daily 8-hour average (MDA8) O_3) and timing of high-O_3 events in the model. The model underestimates the frequency of high events in spring. The ten most biased days (considering regionally-averaged MDA8 O_3 values in each of the ten EPA regions) tend to be around 10°C warmer than average days. Our model does not include daily variations in U.S. anthropogenic emissions associated with higher electricity demand on hotter days (e.g., Abel et al., 2017), but we still find that the influence of U.S. anthropogenic emissions on regionally averaged MDA8 O_3 is up to 30 ppb higher on the ten most biased days as compared to average days. The model does include daily variability in temperature-sensitive biogenic emissions and simulates higher than average O_3 from BVOCs (up to 15 ppb) and soil NO_x (up to 10 ppb) on the ten most biased days. We conclude that regional production of O_3 is driving the pervasive high positive model bias in summer, as opposed to transported background.

On the ten days with the highest observed MDA8 O_3 values (O_3_top10obs) in each season, the model indicates that U.S. anthropogenic and biogenic VOC emissions are the most important drivers relative to average days, over most regions (Tables 3, 4). O_3_top10obs_MAM and O_3_top10obs_SON days (i.e., the ten highest spring and fall MDA8 O_3 days) are up to 9°C warmer, but O_3_top10obs_JJA days (i.e., the ten highest summer MDA8 O_3 days) are only 1-2 °C warmer than average. U.S. anthropogenic emissions enhance O_3_top10obs_JJA days by 5-11 ppb in the eastern U.S. regions, but by less than 2 ppb over the three western regions. Over these westernmost regions, U.S. background O_3 is 4-12 ppb higher on O_3_top10obs_JJA days than on average. Across the continental U.S.A., biogenic VOC emissions enhance O_3 by 1-7 ppb above average on O_3_top10obs_JJA days, while intercontinental pollution is either similar or up to 2 ppb higher on average days. Analysis of our simulations thus indicates that the highest O_3 events are associated with regional O_3 production rather than transported background. We emphasize, however, that our model is likely missing springtime events associated with stratospheric intrusions and Asian transport (Figure 3, Figure 7; Fiore et al., 2014; Zhang et al., 2011; 2014).

From 2004-2012, MDA8 O_3 concentrations on O_3_top10obs_JJA days vary from year-to-year, but show little overall trend (decrease of 3 ppb in both the observations and the model averaged over all regions) (Figure 10, Table 5). With our sensitivity simulations, we interpret this lack of an overall trend as a balance between rising U.S. background O_3 (by 2 ppb for O_3_USB from 2004-2006 to 2010-2012 averaged over all regions) and declining U.S. anthropogenic emissions (by 6 ppb for O_3_USA from 2004-2006 to 2010-2012 averaged over all regions). The declining influence of U.S. anthropogenic emissions on O_3_top10obs_JJA days is consistent with earlier work showing high-O_3 concentrations decreasing in response to regional precursor emissions controls since the late 1990s (e.g. Cooper et al., 2012, 2014b; Frost et al., 2006; Simon et al., 2016).

In contrast to previous work, including with the GEOS-Chem model (e.g. Fiore et al., 2014 and references therein), we find that U.S. background O_3 tends to be higher in summer than in spring in most regions. This likely reflects differences in the isoprene chemistry, specifically the isoprene nitrates, between our version of GEOS-Chem (Mao et al., 2013) and older versions that treat isoprene nitrates as greater sinks for NO_x and thereby, suppress O_3 production. We find here that soil NO_x and isoprene can lead to high U.S. background O_3 in summer, though their relative importance is likely exaggerated at the coarse resolution we use here (e.g., Yu et al., 2016). Nevertheless, the model shows substantial variability in simulated U.S. background O_3 concentrations from year-to-year, on the order of 10-20 ppb between 2004-2012 in summer (Figure 11). The importance of temperature sensitive sources like biogenic VOC and NO_x emissions to background O_3 imply that in a warmer climate, these background influences on O_3 will play an even more important role in driving up O_3 levels.

Acknowledgments

We acknowledge insightful discussions with Gail Tonnesen and Pat Dolwick (U.S. EPA). We gratefully acknowledge support from NASA AQAST (NNX12AF15G) and NASA HAQAST (NNX16AQ20G). This project has been funded in part by the United States Environmental Protection Agency under assistance agreement RD83587801 to AMF. The contents of this document do not necessarily reflect the views and policies of the Environmental Protection Agency, nor does the EPA endorse trade names or recommend the use of commercial products mentioned in this document.

References

Abatzoglou, J. T. and Williams, A. P.: Impact of anthropogenic climate change on wildfire across western US forests, Proc. Natl. Acad. Sci., 113(42), 11770–11775, doi:10.1073/pnas.1607171113, 2016.

Abel, D., Holloway, T., Kladar, R. M., Meier, P., Ahl, D., Harkey, M. and Patz, J.: Response of Power Plant Emissions to Ambient Temperature in the Eastern United States, Environ. Sci. Technol., 51(10), 5838–5846, doi:10.1021/acs.est.6b06201, 2017.

Auvray, M. and Bey, I.: Long-range transport to Europe: Seasonal variations and implications for the European ozone budget, J. Geophys. Res., 110(D11), D11303, doi:10.1029/2004JD005503, 2005.

Barkley, M. P., Palmer, P. I., Ganzeveld, L., Arneth, A., Hagberg, D., Karl, T., Guenther, A., Paulot, F., Wennberg, P. O., Mao, J., Kurosu, T. P., Chance, K., Müller, J. F., De Smedt, I., Van Roozendael, M., Chen, D., Wang, Y. and Yantosca, R. M.: Can a "state of the art" chemistry transport model simulate Amazonian tropospheric chemistry?, J. Geophys. Res. Atmos., 116(16), D16302, doi:10.1029/2011JD015893, 2011.

Baylon, P. M., Jaffe, D. A., Pierce, R. B. and Gustin, M. S.: Interannual Variability in Baseline Ozone and Its Relationship to Surface Ozone in the Western U.S., Environ. Sci. Technol., 50(6), 2994–3001, doi:10.1021/acs.est.6b00219, 2016.

Bond, T. C., Bhardwaj, E., Dong, R., Jogani, R., Jung, S., Roden, C., Streets, D. G. and Trautmann, N. M.: Historical emissions of black and organic carbon aerosol from energy-related combustion, 1850-2000, Global Biogeochem. Cycles, 21(2), 1850–2000, doi:10.1029/2006GB002840, 2007.

Bouwman, A. F., Lee, D. S., Asman, W. A. H., Dentener, F. J., Van Der Hoek, K. W. and Olivier, J. G. J.: A global high-resolution emission inventory for ammonia, Global Biogeochem. Cycles, 11(4), 561–587, doi:10.1029/97GB02266, 1997.

Clifton, O. E., Fiore, A. M., Munger, J. W., Malyshev, S., Horowitz, L. W., Shevliakova, E., Paulot, F., Murray, L. T. and Griffin, K. L.: Interannual variability in ozone removal by a temperate deciduous forest, Geophys. Res. Lett., 44(1), 542–552, doi:10.1002/2016GL070923, 2017.

Cooper, O. R., Gao, R.-S., Tarasick, D., Leblanc, T. and Sweeney, C.: Long-term ozone trends at rural ozone monitoring sites across the United States, 1990-2010, J. Geophys. Res. Atmos., 117(22), n/a-n/a, doi:http://dx.doi.org/10.1029/2012JD018261, 2012.

Cooper, O. R., Parrish, D. D., Ziemke, J., Balashov, N. V., Cupeiro, M., Galbally, I. E., Gilge, S., Horowitz, L., Jensen, N. R., Lamarque, J.-F., Naik, V., Oltmans, S. J., Schwab, J., Shindell, D. T., Thompson, A. M., Thouret, V., Wang, Y. and Zbinden, R. M.: Global distribution and trends of tropospheric ozone: An observation-based review, Elem. Sci. Anthr., 2, 29, doi:10.12952/journal.elementa.000029, 2014a.

Cooper, O. R., Parrish, D. D., Ziemke, J., Balashov, N. V., Cupeiro, M., Galbally, I. E., Gilge, S., Horowitz, L., Jensen, N. R., Lamarque, J.-F., Naik, V., Oltmans, S. J., Schwab, J., Shindell, D. T., Thompson, A. M., Thouret, V., Wang, Y. and Zbinden, R. M.: Global distribution and trends of tropospheric ozone: An observation-based review, Elem. Sci. Anthr., 2(0), 29, doi:10.12952/journal.elementa.000029, 2014b.

Van Donkelaar, A., Martin, R. V, Leaitch, W. R., Macdonald, A. M., Walker, T. W., Streets, D. G., Zhang, Q., Dunlea, E. J., Jimenez, J. L., Dibb, J. E., Huey, L. G., Weber, R. and Andreae, M. O.: Analysis of aircraft and satellite measurements from the Intercontinental Chemical Transport Experiment (INTEX-B) to quantify long-range transport of East Asian sulfur to Canada, Atmos. Chem. Phys. Atmos. Chem. Phys., 8, 2999–3014 [online] Available from: www.atmos-chem-phys.net/8/2999/2008/ (Accessed 23 August 2016), 2008.

Fiore, A. M., Jacob, D. J., Field, B. D., Streets, D. G., Fernandes, S. D. and Jang, C.: Linking ozone pollution and climate change: The case for controlling methane, Geophys. Res. Lett., 29(19), 1919, doi:10.1029/2002GL015601, 2002.

Fiore, A. M., Jacob, D. J., Liu, H., Yantosca, R. M., Fairlie, T. D. and Li, Q.: Variability in surface ozone background over the United States: Implications for air quality policy, J. Geophys. Res., 108(D24), 4787, doi:10.1029/2003jd003855, doi:10.1029/2003jd003855, 2003.

Fiore, A. M., Oberman, J. T., Lin, M., Zhang, L., Clifton, O. E., Jacob, D. J., Naik, V., Horowitz, L. W., Pinto, J. P. and Milly, G. P.: Estimating North American background ozone in U.S. surface air with two independent global models: Variability, uncertainties, and recommendations, Atmos. Environ., 96, 284–300, doi:10.1016/j.atmosenv.2014.07.045, 2014.

Fiore, A. M., Vaishali, N. and Leibensperger, E. M.: Air Quality and Climate Connections, J. Air Waste Manage. Assoc., 2015.

Frost, G. J., McKeen, S. A., Trainer, M., Ryerson, T. B., Neuman, J. A., Roberts, J. M., Swanson, A., Holloway, J. S., Sueper, D. T., Fortin, T., Parrish, D. D., Fehsenfeld, F. C., Flocke, F., Peckham, S. E., Grell, G. A., Kowal, D., Cartwright, J., Auerbach, N. and Habermann, T.: Effects of changing power plant NOx emissions on ozone in the eastern United States: Proof of concept, J. Geophys. Res., 111(D12), D12306, doi:10.1029/2005JD006354, 2006.

Giglio, L., Randerson, J. T., Van Der Werf, G. R., Kasibhatla, P. S., Collatz, G. J., Morton, D. C. and Defries, R. S.: Assessing variability and long-term trends in burned area by merging multiple satellite fire products, Biogeosciences, 7(3), 1171–1186, doi:10.5194/bg-7-1171-2010, 2010.

Guenther, A. B., Jiang, X., Heald, C. L., Sakulyanontvittaya, T., Duhl, T., Emmons, L. K. and Wang, X.: The model of emissions of gases and aerosols from nature version 2.1 (MEGAN2.1): An extended and updated framework for modeling biogenic emissions, Geosci. Model Dev., 5(6), 1471–1492, doi:10.5194/gmd-5-1471-2012, 2012.

Hu, L., Millet, D. B., Baasandorj, M., Griffis, T. J., Travis, K. R., Tessum, C. W., Marshall, J. D., Reinhart, W. F., Mikoviny, T., Müller, M., Wisthaler, A., Graus, M., Warneke, C. and de Gouw, J.: Emissions of C_6-C_8 aromatic compounds in the United States: Constraints from tall tower and aircraft measurements, J. Geophys. Res. Atmos., 120(2), 826–842, doi:10.1002/2014JD022627, 2015.

Hudman, R. C., Moore, N. E., Mebust, A. K., Martin, R. V, Russell, A. R., Valin, L. C. and Cohen, R. C.: Steps towards a mechanistic model of global soil nitric oxide emissions: Implementation and space based-constraints, Atmos. Chem. Phys., 12(16), 7779–7795, doi:10.5194/acp-12-7779-2012, 2012.

Jacob, D. J., Horowitz, L. W., Munger, J. W., Heikes, B. G., Dickerson, R. R., Artz, R. S. and Keene, W. C.: Seasonal transition from NO\~ x-to hydrocarbon-limited conditions for ozone production over the eastern United States in September, J. Geophys. Res., 100, 9315–9315, doi:10.1029/94JD03125, 1995.

Jaffe, D. A.: Relationship between surface and free tropospheric ozone in the Western U.S., Environ. Sci. Technol., 45(2), 432–8, doi:10.1021/es1028102, 2011.

Jaffe, D. A., Cooper, O. R., Fiore, A. M., Henderson, B. H., Gail, S., Russell, A. G., Henze, D. K., Langford, A. O., Lin, M. and Moore, T.: Scientific assessment of background ozone over the U.S.: implications for air quality management, 2017.

Kuhns, H. and Green, M.: Big Bend Regional Aerosol and Visibility Observational (BRAVO) Study Emissions Inventory, Desert Res. …, 89119(702) [online] Available from: http://citeseerx.ist.psu.edu/viewdoc/download?doi=10.1.1.462.8648&rep=rep1&type=pdf (Accessed 29 January 2018), 2003.

Lee, C., Martin, R. V., van Donkelaar, A., Lee, H., Dickerson, R. R., Hains, J. C., Krotkov, N., Richter, A., Vinnikov, K. and Schwab, J. J.: SO_2 emissions and lifetimes: Estimates from inverse modeling using in situ and global, space-based (SCIAMACHY and OMI) observations, J. Geophys. Res., 116(D6), D06304, doi:10.1029/2010JD014758, 2011.

Leibensperger, E. M., Mickley, L. J., Jacob, D. J., Chen, W.-T., Seinfeld, J. H., Nenes, A., Adams, P. J., Streets, D. G., Kumar, N. and Rind, D.: Climatic effects of 1950–2050 changes in US anthropogenic aerosols – Part 2: Climate response, Atmos. Chem. Phys., 12(7), 3349–3362, doi:10.5194/acp-12-3349-2012, 2012.

Lin, M., Fiore, A. M., Cooper, O. R., Horowitz, L. W., Langford, A. O., Levy, H., Johnson, B. J., Naik, V., Oltmans, S. J. and Senff, C. J.: Springtime high surface ozone events over the western United States: Quantifying the role of stratospheric intrusions, J. Geophys. Res. Atmos., 117(D21), doi:10.1029/2012JD018151, 2012.

Lin, M., Fiore, A. M., Horowitz, L. W., Langford, A. O., Oltmans, S. J., Tarasick, D. and Rieder, H. E.: Climate variability modulates western US ozone air quality in spring via deep stratospheric intrusions., Nat. Commun., 6(May), 7105, doi:10.1038/ncomms8105, 2015a.

Lin, M., Horowitz, L. W., Cooper, O. R., Tarasick, D., Conley, S., Iraci, L. T., Johnson, B. J., Leblanc, T., Petropavlovskikh, I. and Yates, E. L.: Revisiting the evidence of increasing springtime ozone mixing ratios in the free troposphere over western North America, Geophys. Res. Lett., 42(20), 8719–8728, doi:10.1002/2015GL065311, 2015b.

Lin, M., Horowitz, L. W., Payton, R., Fiore, A. M. and Tonnesen, G.: US surface ozone trends and extremes from 1980-2014: Quantifying the roles of rising Asian emissions, domestic controls, wildfires, and climate, Atmos. Chem. Phys. Discuss., 1–56, doi:10.5194/acp-2016-1093, 2016.

Mao, J., Horowitz, L. W., Naik, V., Fan, S., Liu, J. and Fiore, A. M.: Sensitivity of tropospheric oxidants to biomass burning emissions: implications for radiative forcing, Geophys. Res. Lett., 40(6), 1241–1246, doi:10.1002/grl.50210, 2013.

National Research Council: Global Sources of Local Pollution: An Assessment of Long-Range Transport of Key Air Pollutants to and from the United States, The National Academies Press, Washington, DC., 2010.

Olivier, J. G. J., Van Aardenne, J. A., Dentener, F. J., Pagliari, V., Ganzeveld, L. N. and Peters, J. A. H. W.: Recent trends in global greenhouse gas emissions:regional trends 1970–2000 and spatial distributionof key sources in 2000, Environ. Sci., 2(2–3), 81–99, doi:10.1080/15693430500400345, 2005.

Reidmiller, D. R., Fiore, A. M., Jaffe, D. A., Bergmann, D., Cuvelier, C., Dentener, F. J., Duncan, B. N., Folberth, G. A., Gauss, M., Gong, S., Hess, P., Jonson, J. E., Keating, T., Lupu, A., Marmer, E., Park, R. J., Schultz, M. G., Shindell, D. T., Szopa, S., Vivanco, M. G., Wild, O. and Zuber, A.: The influence of foreign vs. North American

emissions on surface ozone in the US, Atmos. Chem. Phys., 9(14), 5027–5042, doi:10.5194/acp-9-5027-2009, 2009.
Rienecker, M. M., Suarez, M. J., Gelaro, R., Todling, R., Bacmeister, J., Liu, E., Bosilovich, M. G., Schubert, S. D., Takacs, L., Kim, G. K., Bloom, S., Chen, J., Collins, D., Conaty, A., Da Silva, A., Gu, W., Joiner, J., Koster, R. D., Lucchesi, R., Molod, A., Owens, T., Pawson, S., Pegion, P., Redder, C. R., Reichle, R., Robertson, F. R., Ruddick, A. G., Sienkiewicz, M. and Woollen, J.: MERRA: NASA's modern-era retrospective analysis for research and applications, J. Clim., 24(14), 3624–3648, doi:10.1175/JCLI-D-11-00015.1, 2011.
Schnell, J. L., Holmes, C. D., Jangam, A. and Prather, M. J.: Skill in forecasting extreme ozone pollution episodes with a global atmospheric chemistry model, Atmos. Chem. Phys., 14(15), 7721–7739, doi:10.5194/acp-14-7721-2014, 2014.
Schultz, M. G.: REanalysis of the TROpospheric chemical composition over the past 40 years, Reports Earth Syst. Sci., 48 [online] Available from: http://pubman.mpdl.mpg.de/pubman/item/escidoc:994467/component/escidoc:994466/WEB_BzE_48.pdf (Accessed 29 January 2018), 2007.
Simon, H., Wells, B., Baker, K. R. and Hubbell, B.: Assessing temporal and spatial patterns of observed and predicted ozone in multiple urban areas, Environ. Health Perspect., 124(9), 1443–1452, doi:10.1289/EHP190, 2016.
Stettler, M. E. J., Eastham, S. and Barrett, S. R. H.: Air quality and public health impacts of UK airports. Part I: Emissions, Atmos. Environ., 45, 5415–5424, doi:10.1016/j.atmosenv.2011.07.012, 2011.
Streets, D. G., Zhang, Q., Wang, L., He, K., Hao, J., Wu, Y., Tang, Y. and Carmichael, G. R.: Revisiting China's CO emissions after the Transport and Chemical Evolution over the Pacific (TRACE-P) mission: Synthesis of inventories, atmospheric modeling, and observations, J. Geophys. Res. Atmos., 111(14), D14306, doi:10.1029/2006JD007118, 2006.
Travis, K. R., Jacob, D. J., Keller, C. A., Kuang, S., Lin, J., Newchurch, M. J. and Thompson, A. M.: Resolving ozone vertical gradients in air quality models, Atmos. Chem. Phys. Discuss., 1–18, doi:10.5194/acp-2017-596, 2017.
U.S. Environmental Protection Agency: Map of EPA Regions, [online] Available from: http://www.epa.gov/oust/regions/regmap.htm (Accessed 2 December 2015), 2012.
U.S. Environmental Protection Agency: AirData - Download Data. [online] Available from: http://aqsdr1.epa.gov/aqsweb/aqstmp/airdata/download_files.html#Daily, 2014.
Wang, C., Corbett, J. J. and Firestone, J.: Improving spatial representation of global ship emissions inventories, Environ. Sci. Technol., 42(1), 193–199, doi:10.1021/es0700799, 2008.
Wang, H., Jacob, D. J., Le Sager, P., Streets, D. G., Park, R. J., Gilliland, A. B. and van Donkelaar, A.: Surface ozone background in the United States: Canadian and Mexican pollution influences, Atmos. Environ., 43(6), 1310–1319, doi:10.1016/j.atmosenv.2008.11.036, 2009.
Van Der Werf, G. R., Randerson, J. T., Giglio, L., Collatz, G. J., Mu, M., Kasibhatla, P. S., Morton, D. C., Defries, R. S., Jin, Y. and Van Leeuwen, T. T.: Global fire emissions and the contribution of deforestation, savanna, forest, agricultural, and peat fires (1997-2009), Atmos. Chem. Phys., 10(23), 11707–11735, doi:10.5194/acp-10-11707-2010, 2010.
Xiao, Y., Logan, J. A., Jacob, D. J., Hudman, R. C., Yantosca, R. and Blake, D. R.: Global budget of ethane and regional constraints on U.S. sources, J. Geophys. Res., 113(D21), D21306, doi:10.1029/2007JD009415, 2008.
Yang, J., Tian, H., Tao, B., Ren, W., Pan, S., Liu, Y. and Wang, Y.: A growing importance of large fires in conterminous United States during 1984-2012, J. Geophys. Res. G Biogeosciences, 120(12), 2625–2640, doi:10.1002/2015JG002965, 2015.
Yevich, R. and Logan, J. A.: An assessment of biofuel use and burning of agricultural waste in the developing world, Global Biogeochem. Cycles, 17(4), n/a-n/a, doi:10.1029/2002GB001952, 2003.
Young, P. J., Naik, V., Fiore, A. M., Gaudel, A., Guo, J., Lin, M. Y., Neu, J., Parrish, D. D., Rieder, H. E., Schnell, J. L., Tilmes, S., Wild, O., Zhang, L., Brandt, J., Delcloo, A., Doherty, R. M., Geels, C., Hegglin, M. I., Hu, L., Im, U., Kumar, R., Luhar, A., Murray, L. T., Plummer, D., Rodriguez, J., Saiz-Lopez, A., Schultz, M. G., Woodhouse, M., Zeng, G. and Ziemke, J.: Tropospheric Ozone Assessment Report (TOAR): Assessment of global-scale model performance for global and regional ozone distributions, variability, and trends, Elem. Sci. Anthr., 0–84 [online] Available from: http://eprints.lancs.ac.uk/88836/1/TOAR_Model_Performance_07062017.pdf (Accessed 12 December 2017), 2017.
Yu, K., Jacob, D. J., Fisher, J. A., Kim, P. S., Marais, E. A., Miller, C. C., Travis, K. R., Zhu, L., Yantosca, R. M., Sulprizio, M. P., Cohen, R. C., Dibb, J. E., Fried, A., Mikoviny, T., Ryerson, T. B., Wennberg, P. O. and Wisthaler, A.: Sensitivity to grid resolution in the ability of a chemical transport model to simulate observed oxidant chemistry under high-isoprene conditions, Atmos. Chem. Phys, 16, 4369–4378, doi:10.5194/acp-16-4369-2016, 2016.
Zhang, L., Jacob, D. J., Downey, N. V., Wood, D. A., Blewitt, D., Carouge, C. C., van Donkelaar, A., Jones, D. B. A., Murray, L. T. and Wang, Y.: Improved estimate of the policy-relevant background ozone in the United States

using the GEOS-Chem global model with 1/2° × 2/3° horizontal resolution over North America, Atmos. Environ., 45(37), 6769–6776, doi:10.1016/j.atmosenv.2011.07.054, 2011.
Zhang, L., Jacob, D. J., Yue, X., Downey, N. V., Wood, D. A. and Blewitt, D.: Sources contributing to background surface ozone in the US Intermountain West, Atmos. Chem. Phys., 14(11), 5295–5309, doi:10.5194/acp-14-5295-2014, 2014.

Atmos. Chem. Phys. Discuss., https://doi.org/10.5194/acp-2018-115
Manuscript under review for journal Atmos. Chem. Phys.
Discussion started: 26 February 2018

585 **Figures**

Table 1: Approach for estimating sources of ground-level O_3 with the GEOS-Chem model.

Ozone Source	*Definition*	*Notation*
Base	Standard simulation	O_3_Base
Natural Background	Simulation with no global anthropogenic emissions + preindustrial CH_4 levels	O_3_NAT
North American Background	Simulation with no North American anthropogenic emissions	O_3_NAB
U.S. Background	Simulation with no U.S. anthropogenic emissions	O_3_USB
U.S. Anthropogenic Emissions	O_3_Base – O_3_USB	O_3_USA
Anthropogenic Emissions from Canada and Mexico	O_3_USB – O_3_NAB	O_3_CA+MX
Intercontinental Transport + Preindustrial CH_4 Levels	O_3_NAB – O_3_NAT	O_3_ICT+CH_4
North American Lightning NO_x	O_3_Base – simulation with the lightning NO_x source shut off	O_3_NALNO$_x$
Soil NO_x Emissions	O_3_Base – simulation with the soil NO_x emissions shut off	O_3_SNO$_x$
Terrestrial Biogenic VOC Emissions	O_3_Base – simulation with the terrestrial biogenic emissions shut off	O_3_BVOC
All Emissions except Terrestrial Biogenic VOCs	No terrestrial biogenic VOC emissions	O_3_noBVOC
Biomass Burning Emissions	O_3_Base – simulation with biomass burning emissions (NO_x, CO, VOCs, aerosols, and precursors from fires) shut off	O_3_BB

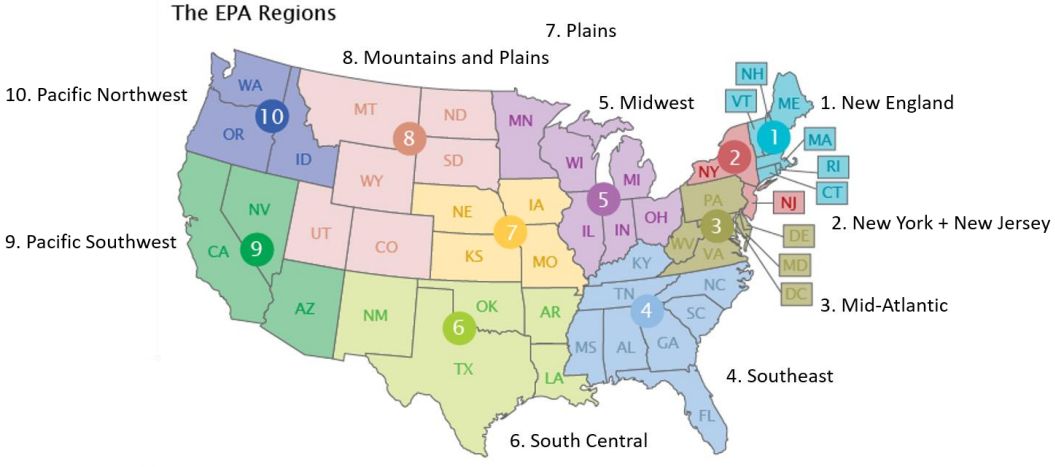

590 **Figure 1: Map of the states falling within each EPA region in the continental United States (adapted from *U.S. Environmental Protection Agency*, 2012).**

Atmos. Chem. Phys. Discuss., https://doi.org/10.5194/acp-2018-115
Manuscript under review for journal Atmos. Chem. Phys.
Discussion started: 26 February 2018

Atmospheric Chemistry and Physics Discussions

Table 2: The number of observational sites that fall within each EPA region for EPA AQS and CASTNet. (*) We include data from the Mount Bachelor Observatory in the Pacific Northwest region.

Region	**EPA AQS**	**CASTNet**	***Total***
1. New England	82	7	*89*
2. New York + New Jersey (NY+NJ)	61	7	*68*
3. Mid-Atlantic	138	14	*152*
4. Southeast	309	24	*333*
5. Midwest	255	18	*273*
6. South Central	202	5	*207*
7. Plains	71	2	*73*
8. Mountains and Plains	153	12	*165*
9. Pacific Southwest	325	14	*339*
10. Pacific Northwest	48	6*	*54*
Total	***1644***	***109***	***1753***

595

Atmos. Chem. Phys. Discuss., https://doi.org/10.5194/acp-2018-115
Manuscript under review for journal Atmos. Chem. Phys.
Discussion started: 26 February 2018

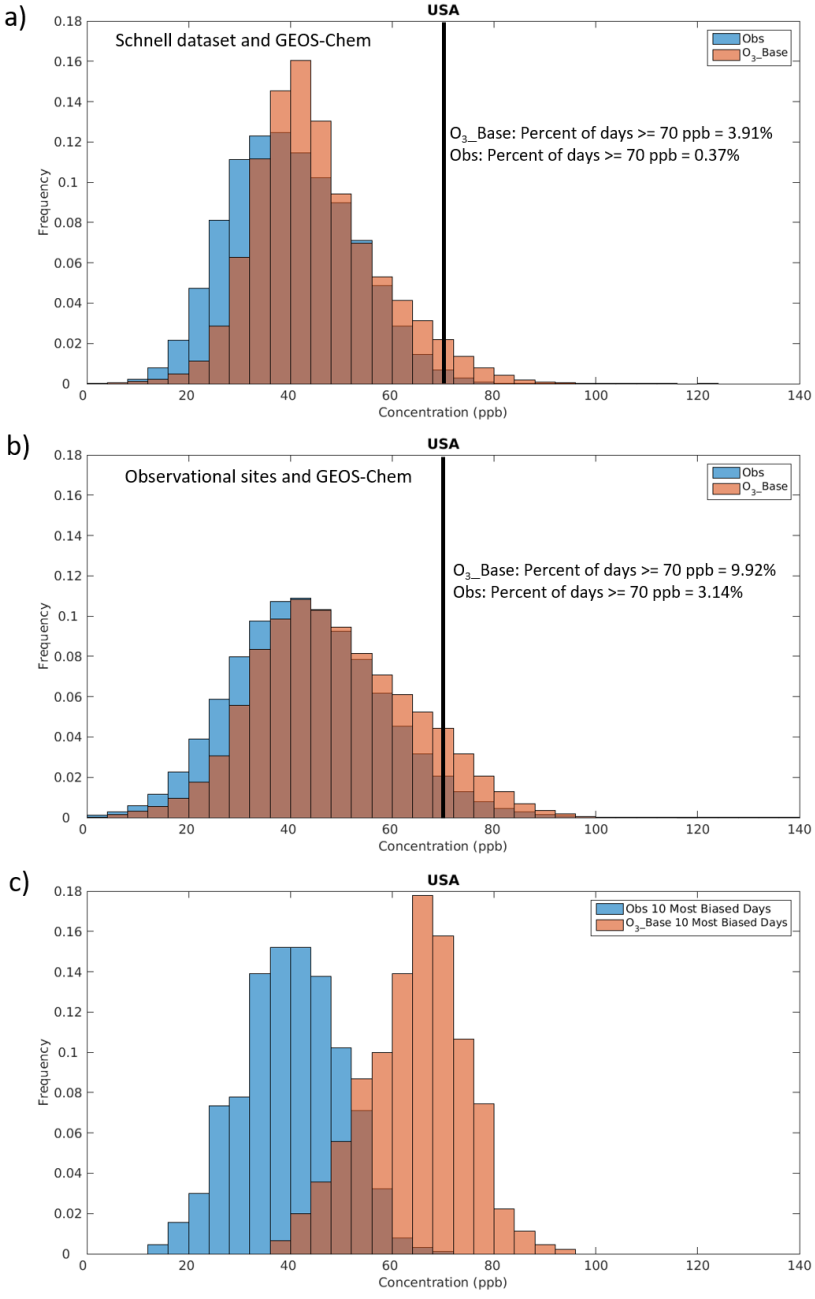

Figure 2: Frequency distribution of MDA8 O_3 values across all sites in the United States from Jan-Dec (365 or 366 days per year) from 2004-2012 in the (a) Schnell dataset (2014) interpolated to 2° by 2.5°, (b) at individual observational sites, and c) on the 10 most biased days. Concentrations for each day are obtained by averaging across all sites in a region. The model bias is defined as O_3_Base minus observed. The total number of points consists of 9 years x 10 days x 10 regions. The observations are in shown in blue and GEOS-Chem is in orange. The line drawn at 70 ppb in panels (a) and (b) denotes the 70 ppb NAAQS standard cut-off for O_3.

Atmos. Chem. Phys. Discuss., https://doi.org/10.5194/acp-2018-115
Manuscript under review for journal Atmos. Chem. Phys.
Discussion started: 26 February 2018

Atmospheric Chemistry and Physics Discussions

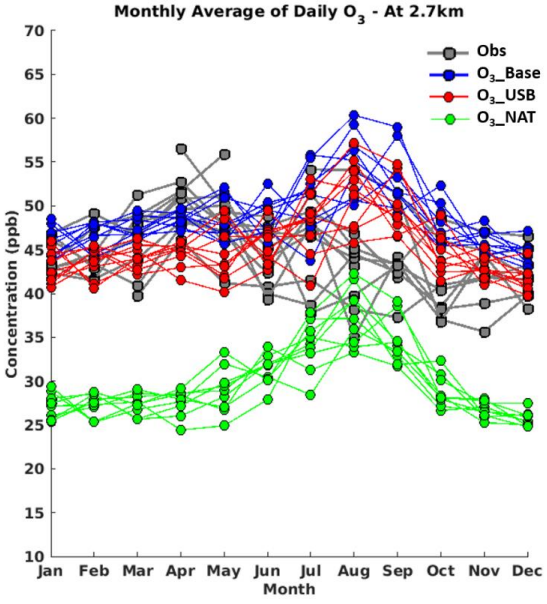

605

Figure 3: Monthly average concentrations of daily O_3 at Mount Bachelor Observatory (Observations; grey), with corresponding O_3_Base (blue), O_3_USB (red), and O_3_NAT (green) concentrations at ~2.7 km, the height of the Mount Bachelor Observatory. Individual lines of the same color show the spread from 2004-2012.

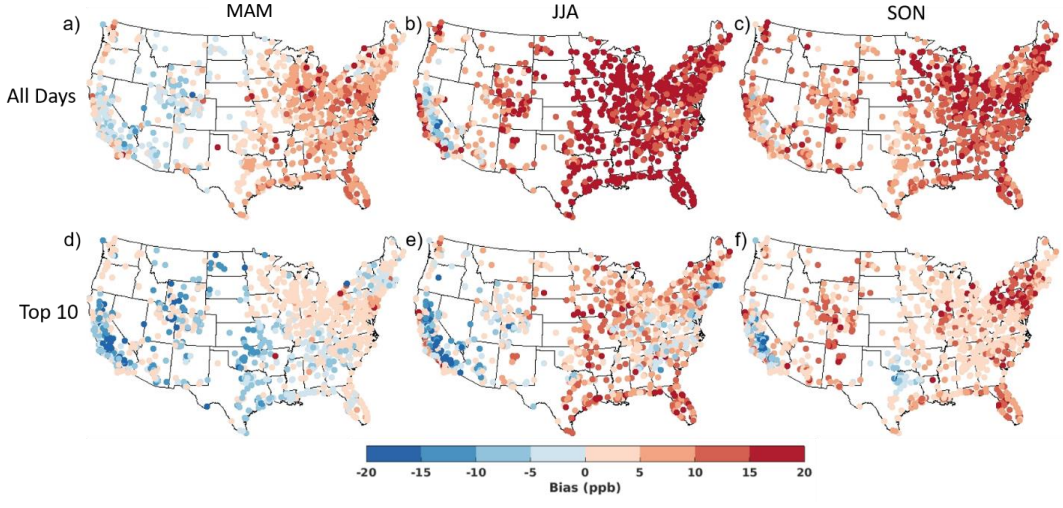

610

Figure 4: Average MDA8 O_3 model bias (O_3_Base – observed) on all days in (a) JJA, (b) MAM, and (c) SON versus on the (d) O_3_top10obs_MAM, (e) O_3_top10obs_JJA, and (f) O_3_top10obs_SON days at each observational site averaged across 2004-2012.

Atmos. Chem. Phys. Discuss., https://doi.org/10.5194/acp-2018-115
Manuscript under review for journal Atmos. Chem. Phys.
Discussion started: 26 February 2018

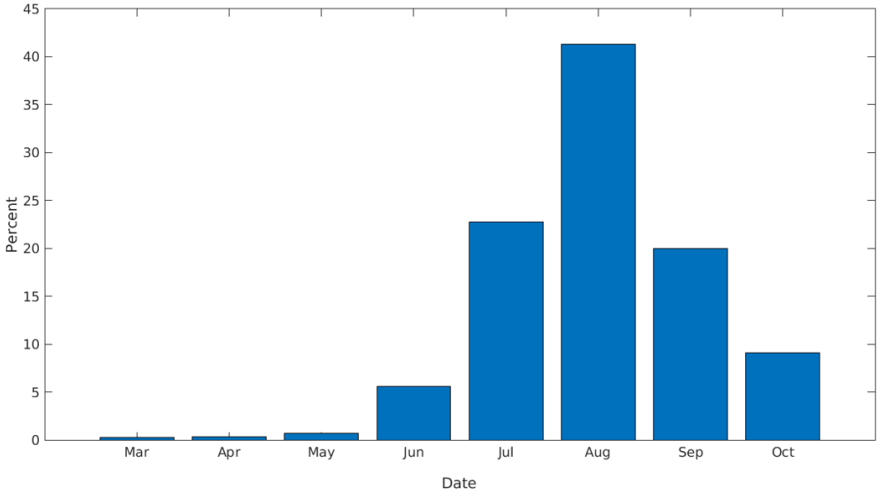

615 **Figure 5: Percent of total top 10 most biased days from Jan-Dec (9 years x 10 days x 10 regions) that fell within each month in the United States. All the most biased days fell between Mar-Oct.**

620

Atmos. Chem. Phys. Discuss., https://doi.org/10.5194/acp-2018-115
Manuscript under review for journal Atmos. Chem. Phys.
Discussion started: 26 February 2018

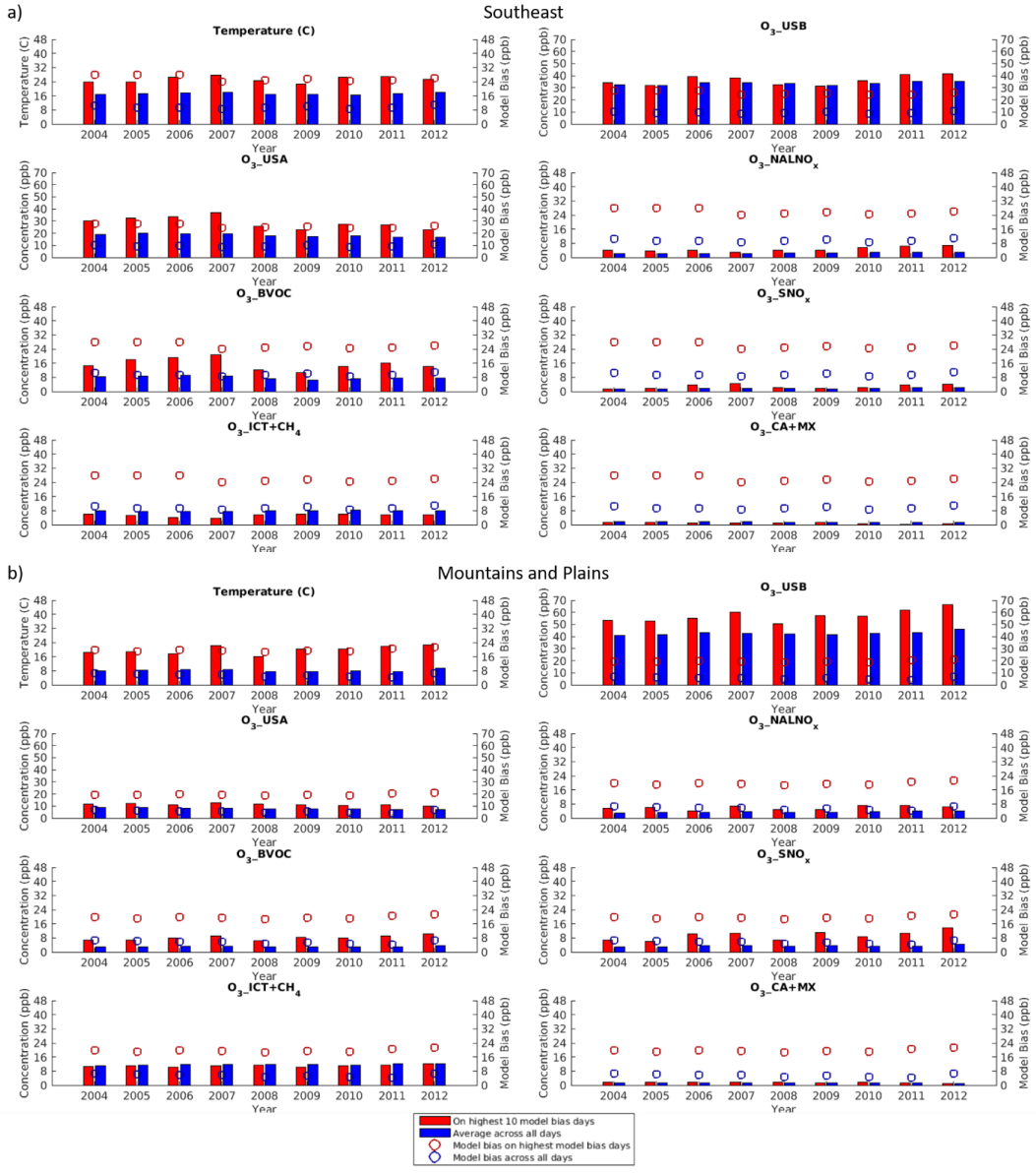

Figure 6: Average influence of each sensitivity simulation on MDA8 O_3 in the (a) Southeast and (b) Mountain and Plains regions on the 10 most biased days from Jan-Dec (red) versus averaged across all days (blue). Red circles show the average model bias (O_3_Base – observations) on the 10 most biased days. Blue circles show the model bias averaged across all days. The circles do not vary between subplots. Note that O_3_USB and O_3_USA are on a different scale than the other plots.

Atmos. Chem. Phys. Discuss., https://doi.org/10.5194/acp-2018-115
Manuscript under review for journal Atmos. Chem. Phys.
Discussion started: 26 February 2018

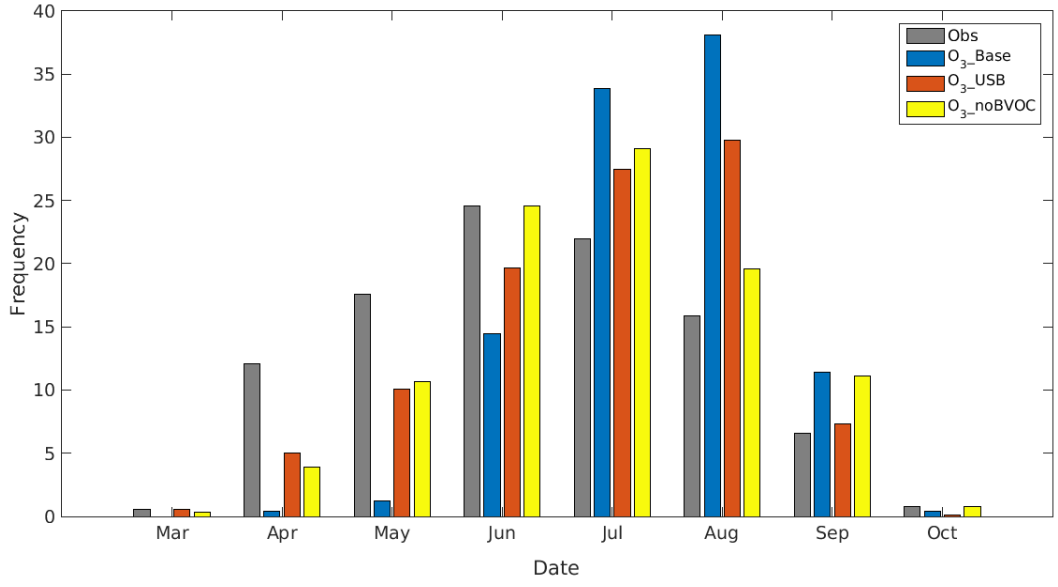

Figure 7: Percent of total top ten days (9 years x 10 days x 10 regions) from Jan-Dec (365 or 366 days) in the observations, O_3_Base, O_3_USB, and O_3_noBVOC that fell within each month for all sites across the U.S.A. All the top ten days for each simulation fell between Mar-Oct.

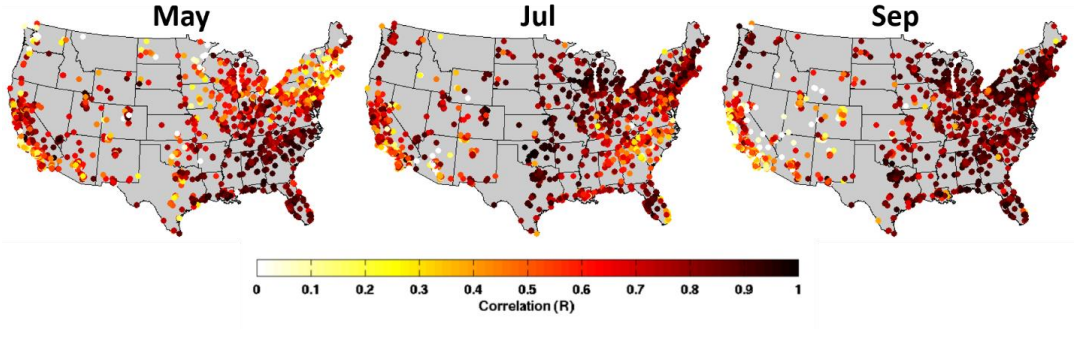

Figure 8: Correlation between 2004-2012 year-to-year monthly MDA8 O_3 averages for May, July, and September in the observation and in the model (O_3_Base).

Atmos. Chem. Phys. Discuss., https://doi.org/10.5194/acp-2018-115
Manuscript under review for journal Atmos. Chem. Phys.
Discussion started: 26 February 2018

Atmospheric Chemistry and Physics Discussions

Table 3: Summary information for each region. The "Model Bias" column shows the model bias in each region on the (1) O_3_top10obs days in each season (average of 2004-2012), 2) across all days in each season (average of 2004-2012), and (3) the difference between these values, rounded to the nearest whole number. The other columns show the concentration for the observations, O_3_Base, and O_3_USA, and daily average temperature (in degrees C) on the (1) O_3_top10obs days in each season (average of 2004-2012), (2) across all days in each season (average of 2004-2012), and (3) the difference between these values.

	Metric	Model Bias			O_3_Base			Obs			O_3_USB			O_3_USA			Temperature (C)		
Region	*Season*	*MAM*	*JJA*	*SON*	*MAM*	*JJA*	*SON*	*MAM*	*JJA*	*SON*	*MAM*	*JJA*	*SON*	*MAM*	*JJA*	*SON*	*MAM*	*JJA*	*SON*
New England	Top 10 Days	-1	9	12	57	72	59	58	62	59	35	39	36	22	33	23	12	22	18
	Avg all days	2	14	10	46	56	41	44	43	31	35	35	32	12	21	9	7	19	11
	Difference	**-3**	**-4**	**2**	**11**	**16**	**18**	**13**	**20**	**28**	**0**	**4**	**3**	**10**	**11**	**14**	**5**	**2**	**6**
NY+NJ	Top 10 Days	4	14	15	63	80	65	59	67	65	36	42	38	27	38	27	16	24	20
	Avg all days	5	18	11	49	65	42	44	47	31	35	39	33	14	27	10	9	21	12
	Difference	**-1**	**-5**	**4**	**14**	**15**	**23**	**15**	**19**	**34**	**1**	**3**	**6**	**13**	**11**	**18**	**6**	**2**	**7**
Mid-Atlantic	Top 10 Days	3	13	15	65	81	69	63	68	69	34	40	37	31	40	32	18	25	21
	Avg all days	6	18	12	51	70	45	46	52	33	34	38	32	17	32	13	12	23	14
	Difference	**-3**	**-5**	**3**	**14**	**11**	**24**	**17**	**16**	**36**	**0**	**2**	**5**	**14**	**9**	**19**	**6**	**2**	**7**
Southeast	Top 10 Days	0	13	10	62	72	63	61	59	63	34	39	34	27	34	28	19	26	21
	Avg all days	6	19	12	55	65	51	48	46	39	34	37	32	21	28	19	17	26	18
	Difference	**-6**	**-6**	**-1**	**7**	**7**	**12**	**13**	**13**	**24**	**1**	**2**	**3**	**7**	**5**	**10**	**2**	**1**	**3**
Midwest	Top 10 Days	4	14	17	63	77	70	59	63	70	36	44	42	27	33	27	17	24	21
	Avg all days	6	19	11	49	68	43	44	48	32	34	42	33	15	26	10	10	22	12
	Difference	**-1**	**-5**	**6**	**14**	**10**	**26**	**15**	**15**	**37**	**1**	**2**	**9**	**12**	**8**	**17**	**7**	**1**	**9**
South Central	Top 10 Days	0	13	9	60	75	67	60	62	67	39	45	40	21	30	26	20	27	23
	Avg all days	5	17	10	52	62	51	47	46	41	36	41	35	16	21	16	18	27	19
	Difference	**-5**	**-4**	**-2**	**8**	**12**	**15**	**14**	**16**	**26**	**3**	**4**	**5**	**6**	**9**	**10**	**2**	**1**	**4**
Plains	Top 10 Days	0	13	13	58	74	67	58	61	67	37	47	42	21	28	25	17	26	22
	Avg all days	5	18	10	50	67	45	44	49	35	34	44	34	15	23	11	13	25	13
	Difference	**-6**	**-5**	**3**	**8**	**8**	**23**	**14**	**13**	**33**	**2**	**3**	**9**	**6**	**5**	**14**	**4**	**1**	**9**
Mountains + Plains	Top 10 Days	-1	8	13	56	69	64	57	60	64	45	57	54	11	12	10	12	22	18
	Avg all days	0	11	9	50	64	48	50	53	39	41	53	41	10	11	7	7	20	9
	Difference	**-1**	**-2**	**4**	**6**	**5**	**16**	**7**	**7**	**25**	**5**	**4**	**12**	**1**	**0**	**3**	**5**	**2**	**9**
Pacific SW	Top 10 Days	-3	3	6	57	64	63	60	62	63	41	47	48	16	18	15	18	25	24
	Avg all days	0	4	8	49	57	49	49	53	42	37	41	39	12	16	10	14	23	17
	Difference	**-3**	**-1**	**-2**	**8**	**7**	**14**	**10**	**9**	**21**	**4**	**6**	**8**	**4**	**2**	**5**	**5**	**2**	**7**
Pacific NW	Top 10 Days	-1	6	11	48	59	51	49	52	51	39	49	44	9	10	7	12	22	17
	Avg all days	2	8	10	43	46	40	41	38	30	35	36	36	8	10	4	8	17	10
	Difference	**-3**	**-2**	**0**	**5**	**13**	**11**	**9**	**14**	**21**	**4**	**12**	**9**	**1**	**0**	**3**	**4**	**4**	**7**

Atmos. Chem. Phys. Discuss., https://doi.org/10.5194/acp-2018-115
Manuscript under review for journal Atmos. Chem. Phys.
Discussion started: 26 February 2018

Atmospheric Chemistry and Physics Discussions

Table 4: Summary information for each region. Each column shows the concentration for each background O_3 source influence on the (1) O_3_top10obs days in each season (average of 2004-2012), (2) across all days in each season (average of 2004-2012), and (3) the difference between these values, rounded to the nearest whole number.

	Metric	O_3_USB			O_3_BVOC			O_3_SNO_x			O_3_$NALNO_x$			O_3_ICT+CH_4			O_3_CA+MX		
Region	**Season**	**MAM**	**JJA**	**SON**	**MAM**	**JJA**	**SON**	**MAM**	**JJA**	**SON**	**MAM**	**JJA**	**SON**	**MAM**	**JJA**	**SON**	**MAM**	**JJA**	**SON**
New England	Top 10 Days	35	39	36	6	17	13	1	3	2	1	2	1	8	3	5	7	7	5
	Avg all days	35	35	32	2	10	6	1	3	2	1	2	2	10	4	7	6	6	4
	Difference	**0**	**4**	**3**	**4**	**7**	**8**	**0**	**0**	**1**	**0**	**0**	**0**	**-2**	**-1**	**-3**	**1**	**1**	**2**
NY+NJ	Top 10 Days	36	42	38	9	20	17	1	4	3	1	2	2	7	2	4	6	6	5
	Avg all days	35	39	33	3	14	7	1	3	2	1	2	2	10	4	7	5	6	4
	Difference	**1**	**3**	**6**	**6**	**6**	**9**	**0**	**0**	**1**	**0**	**0**	**0**	**-2**	**-1**	**-3**	**1**	**0**	**2**
Mid-Atlantic	Top 10 Days	34	40	37	10	20	18	1	4	3	1	3	2	7	3	5	4	3	4
	Avg all days	34	38	32	5	16	9	1	3	2	1	3	2	9	4	7	4	4	3
	Difference	**0**	**2**	**5**	**5**	**4**	**9**	**0**	**1**	**1**	**0**	**0**	**0**	**-2**	**-1**	**-2**	**0**	**0**	**1**
Southeast	Top 10 Days	34	39	34	7	16	14	2	4	2	1	3	2	8	4	6	2	2	2
	Avg all days	34	37	32	5	14	9	1	3	2	2	4	2	9	5	7	2	1	2
	Difference	**1**	**2**	**3**	**2**	**2**	**4**	**0**	**1**	**1**	**-1**	**-1**	**0**	**0**	**-1**	**-1**	**0**	**1**	**0**
Midwest	Top 10 Days	36	44	42	8	16	16	2	6	5	1	2	2	6	1	4	3	3	3
	Avg all days	34	42	33	3	13	8	1	6	2	1	2	2	9	2	6	4	3	2
	Difference	**1**	**2**	**9**	**4**	**3**	**8**	**1**	**0**	**2**	**0**	**0**	**0**	**-3**	**-1**	**-3**	**0**	**0**	**1**
South Central	Top 10 Days	39	45	40	6	17	14	3	5	4	2	4	2	8	5	6	3	2	2
	Avg all days	36	41	35	4	12	8	2	4	2	2	6	2	9	7	8	3	2	2
	Difference	**3**	**4**	**5**	**2**	**5**	**6**	**1**	**1**	**2**	**0**	**-2**	**0**	**-1**	**-2**	**-2**	**0**	**0**	**0**
Plains	Top 10 Days	37	47	42	5	16	14	3	8	6	1	3	2	7	2	4	3	1	1
	Avg all days	34	44	34	3	13	7	2	8	3	1	3	2	8	3	7	3	2	2
	Difference	**2**	**3**	**9**	**2**	**3**	**7**	**1**	**0**	**3**	**0**	**0**	**0**	**-1**	**-1**	**-2**	**0**	**0**	**0**
Mountains + Plains	Top 10 Days	45	57	54	1	8	7	3	9	7	3	5	5	12	11	12	2	1	1
	Avg all days	41	53	41	1	7	4	2	8	3	2	5	4	12	11	12	2	2	1
	Difference	**5**	**4**	**12**	**1**	**1**	**3**	**1**	**1**	**4**	**1**	**0**	**1**	**0**	**1**	**1**	**0**	**0**	**0**
Pacific SW	Top 10 Days	41	47	48	3	9	9	3	5	5	2	4	4	11	8	10	2	2	2
	Avg all days	37	41	39	1	7	5	1	4	3	2	4	3	12	8	11	1	2	2
	Difference	**4**	**6**	**8**	**2**	**2**	**4**	**1**	**1**	**2**	**0**	**0**	**1**	**-1**	**0**	**-1**	**0**	**0**	**0**
Pacific NW	Top 10 Days	39	49	44	0	9	7	2	7	5	1	3	3	12	9	10	3	4	2
	Avg all days	35	36	36	-1	4	3	1	4	2	1	2	3	13	9	10	2	3	1
	Difference	**4**	**12**	**9**	**1**	**5**	**4**	**1**	**3**	**3**	**0**	**1**	**0**	**0**	**0**	**0**	**1**	**1**	**1**

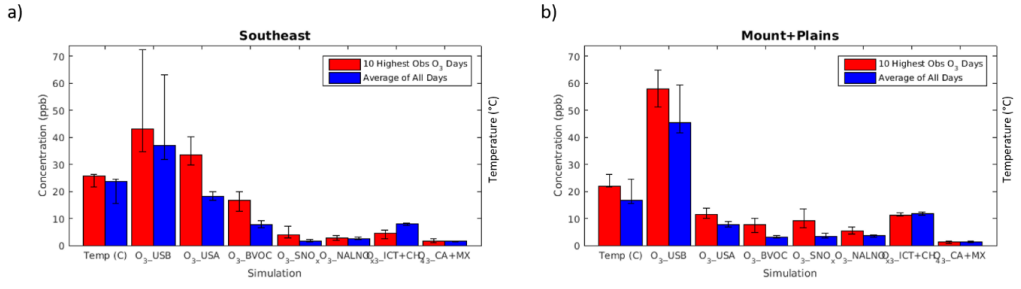

Figure 9: Average 2004-2012 influence of each sensitivity simulation to O_3_Base in the (a) Southeast and (b) Mountains and Plains regions on MDA8 O_3_top10obs_JJA days (red) versus averaged across all days (blue). Error bars show the concentration on the lowest versus highest year for each sensitivity simulation in each region.

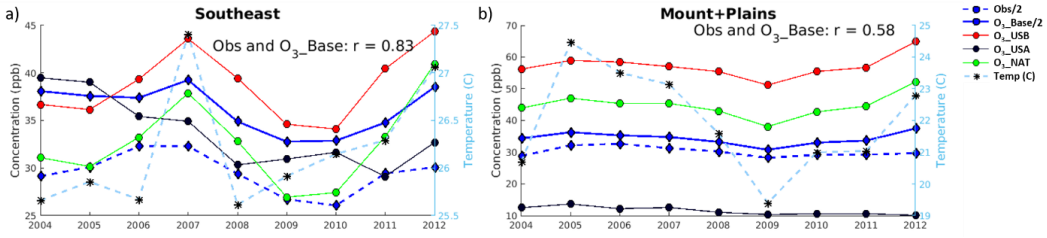

675 **Figure 10: Average yearly MDA8 O_3_top10obs_JJA concentrations for observations (divided by 2 to fit on the same axes; blue dashed line), O_3_Base (divided by 2; blue solid line), O_3_USB (red), O_3_USA (black), O_3_NAT (green) MDA8, and daily average temperature (in degrees C; light blue) in the (a) Southeast and (b) Mountains and Plains regions.**

Table 5: Change in MDA8 O_3 concentrations from 2004-2006 to 2010-2012 on O_3_top10obs_JJA days in the observations, O_3_Base, O_3_USB, and O_3_USA.

	Obs	O_3_Base	O_3_USB	O_3_USA
New England	-6	-4	6	-10
NY+NJ	-2	-4	3	-7
Mid-Atlantic	0	-3	4	-7
Southeast	-4	-5	2	-7
Midwest	-2	-4	2	-6
South Central	-6	-2	5	-7
Plains	-1	-2	4	-5
Mountains + Plains	-4	-1	1	-2
Pacific SW	-3	-4	0	-4
Pacific NW	-7	-5	-4	-1
Average	***-3***	***-3***	***2***	***-6***

Atmos. Chem. Phys. Discuss., https://doi.org/10.5194/acp-2018-115
Manuscript under review for journal Atmos. Chem. Phys.
Discussion started: 26 February 2018

Atmospheric Chemistry and Physics Discussions

680

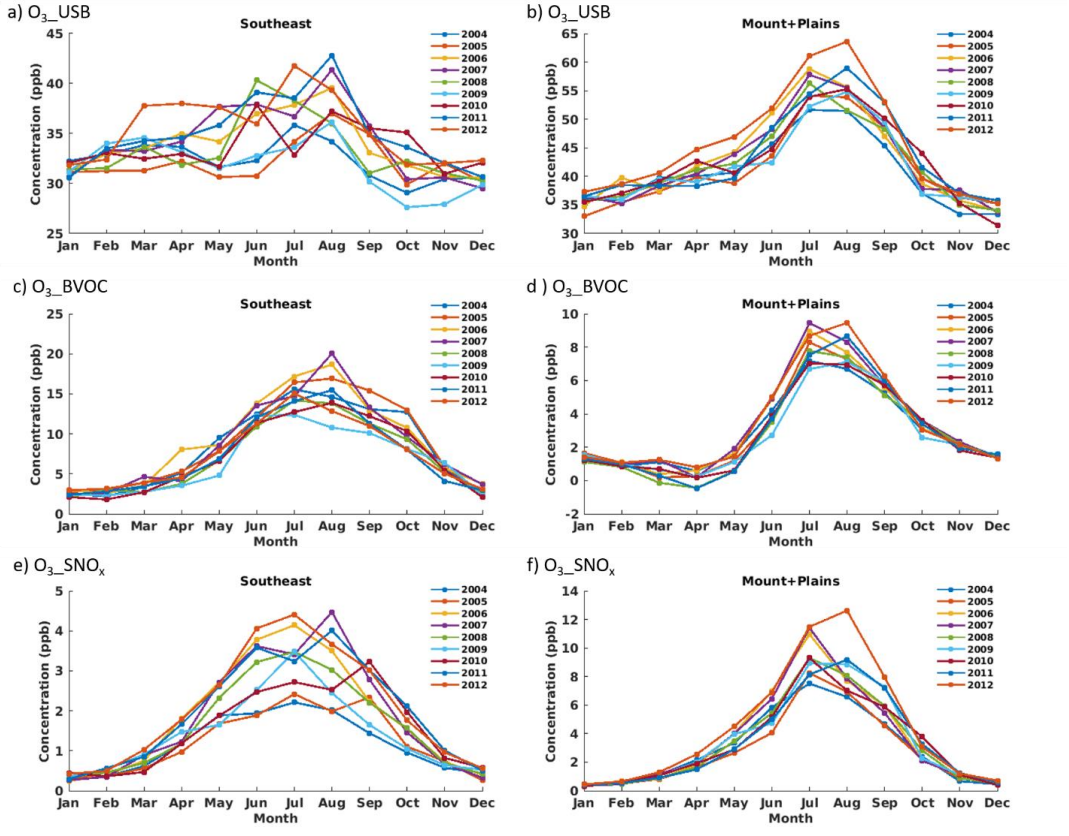

Figure 11: Monthly average MDA8 O_3_USB (a, b), O_3_BVOC (c, d), and O_3_SNO_x (e, f) concentrations in the Southeast (a, c, e) and Mountains and Plains (b, d, f) regions.

Atmos. Chem. Phys. Discuss., https://doi.org/10.5194/acp-2018-115
Manuscript under review for journal Atmos. Chem. Phys.
Discussion started: 26 February 2018

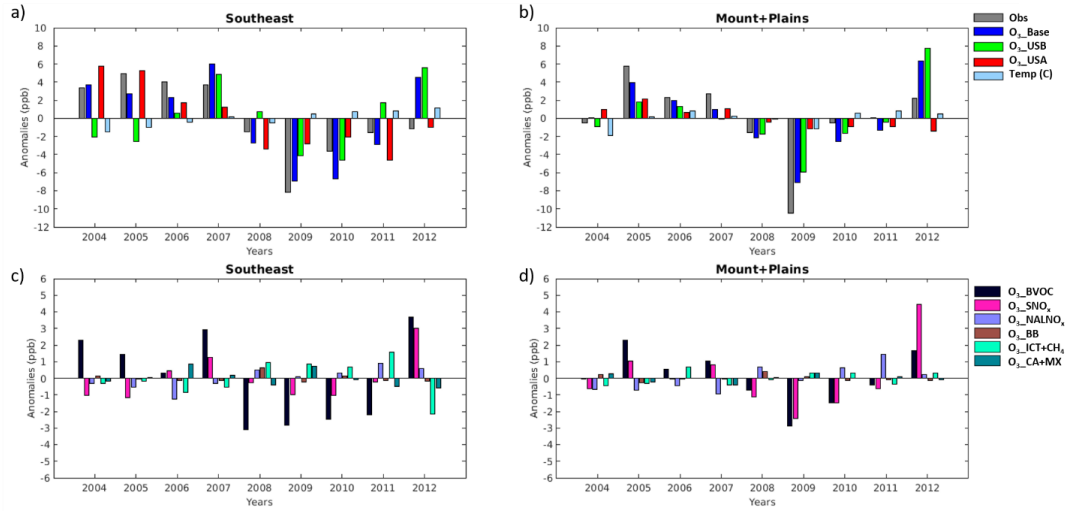

685 **Figure 12: Anomaly on the MDA8 O_3_top10obs_JJA days relative to the 2004-2012 average in the Southeast (a, c) and in the Mountains and Plains (b, d) regions. Panels (a) and (b) show the observations, O_3_Base, O_3_USB, O_3_USA, and temperature (in degrees C). Panels (c) and (d) show O_3_BVOC, O_3_SNO_x, O_3_$NALNO_x$, O_3_BB, O_3_ICT+CH_4, and O_3_CA+MX.**

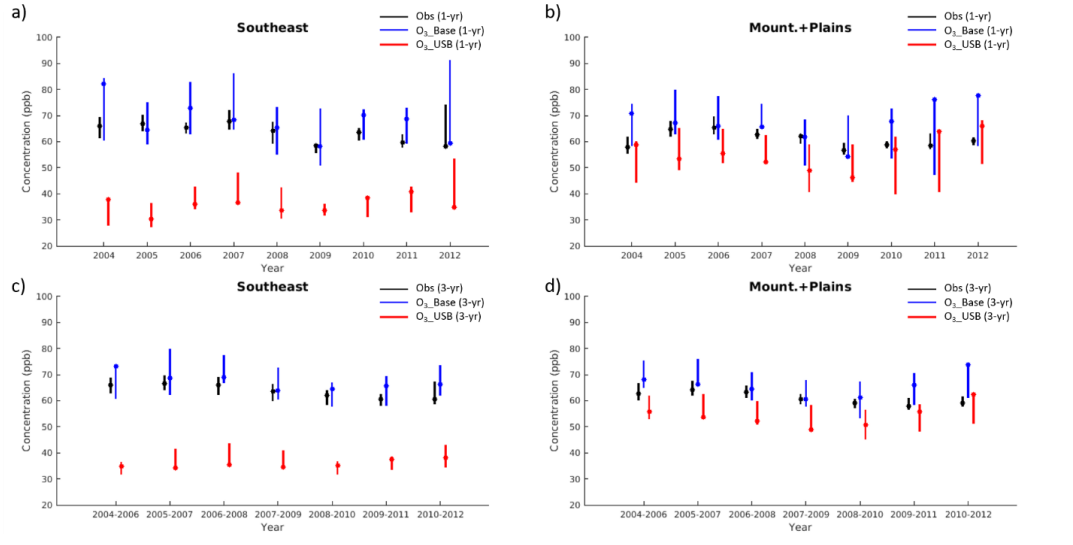

690 **Figure 13: Range in magnitude of the MDA8 O_3_top10obs for each year shown as vertical lines in the observations (black), O_3_Base (blue), and O_3_USB (red) in the (a, c) Southeast and (b, d) Mountains and Plains regions. (a, b) show the range on of O_3_top10obs days during each year between 2004-2012. (c, d) show the range of the O_3_top10obs days after averaging over three consecutive years. The solid dots show the 4th highest MDA8 O_3 day for each simulation (a, b) and the annual 4th highest MDA8 O_3 day averaged over three consecutive years.**

695